Articles in PresS. Physiol Genomics (May 21, 2013). doi:10.1152/physiolgenomics.00034.2013

Title:

Intra-Uterine Calorie Restriction Affects Placental DNA Methylation and Gene Expression

Pao-Yang Chen[1], Amit Ganguly[2], Liudmilla Rubbi[3], Luz D. Orozco[3], Marco Morselli[3], Davin Ashraf[3], Artur Jaroszewicz[3], Suhua Feng[3], Steve E. Jacobsen[3,4], Atsushi Nakano[3,5,6,7], Sherin U. Devaskar[2] & Matteo Pellegrini[3,5,6,8*]

Affiliations

1. Institute of Plant and Microbial Biology, Academia Sinica, Taipei 11529, Taiwan
2. Department of Pediatrics, Division of Neonatology and Developmental Biology, Neonatal Research Center, David Geffen School of Medicine, University of California Los Angeles, Los Angeles, California 90095, USA
3. Department of Molecular, Cell, and Developmental Biology, University of California, Los Angeles, California 90095 USA
4. Howard Hughes Medical Institute, University of California, Los Angeles, Los Angeles, CA 90095, USA
5. Broad Center of Regenerative Medicine and Stem Cell Research, University of California, Los Angeles, Los Angeles, California 90095, USA
6. Molecular Biology Institute, University of California, Los Angeles, California 90095 USA
7. Jonsson Comprehensive Cancer Center, Los Angeles, California 90095 USA
8. Institute of Genomics and Proteomics, University of California, Los Angeles, California 90095 USA

*Corresponding author

Corresponding author:
Matteo Pellegrini
matteop@mcdb.ucla.edu
Office Phone: (310) 825-0012
FAX: (310) 206-3987

Keywords

Intrauterine growth restriction, DNA methylation, placentas, caloric restriction

Abstract

Maternal nutrient restriction causes the development of adult onset chronic diseases in the intra-uterine growth restricted (IUGR) fetus. Investigations in mice have shown that either protein or calorie restriction during pregnancy leads to glucose intolerance, increased fat mass and hypercholesterolemia in adult male offspring. Some of these phenotypes are shown to persist in successive generations. The molecular mechanisms underlying IUGR remain unclear. The placenta is a critical organ for mediating changes in the environment and the development of embryos. To shed light on molecular mechanisms that might affect placental responses to differing environments we examined placentas from mice that had been exposed to different diets. We measured gene expression, and whole genome DNA methylation in both male and female placentas of mice exposed to either caloric restriction or ad libitum diets. We observed several differentially expressed pathways associated with IUGR phenotypes, and, most importantly, a significant decrease in the overall methylation between these groups as well as sex-specific effects that are more pronounced in males. In addition, a set of significantly differentially methylated genes that are enriched for known imprinted genes were identified, suggesting that imprinted loci may be particularly susceptible to diet effects. Lastly, we identified several differentially methylated microRNAs that target genes associated with immunological, metabolic, gastrointestinal, cardiovascular and neurological chronic diseases, as well as genes responsible for trans-placental nutrient transfer and fetal development.

Introduction

Maternal nutrient restriction of the fetus is known to increase the risk of eventually developing adult onset chronic diseases. Investigations in mice related to either protein or calorie restriction have shown that this nutrient deficiency leads to glucose intolerance, increased fat mass and hypercholesterolemia in adult male offspring (7). In humans, suboptimal intrauterine nutrient environments, such as maternal malnutrition or placental disease that interferes with the fetal growth potential, have been linked to an increased incidence of metabolic and cardiovascular disease (9).

While much is known about the phenotypic consequences of the effects of maternal diet during gestation, the underlying molecular mechanisms that are responsible for these are still poorly understood. However, it is thought that the placenta, which is the critical organ for transporting nutrients from the maternal blood to the embryo, must play a critical role in IUGR. In-utero placentas are sensitive to the immediate environment, thereby contributing towards programming that affects the health, growth and survival of the developing fetus (37). Because of its centrality for mediating maternal nutrition effects, several studies have focused on the response of placental gene expression to differing maternal diets. One such study measured placental gene expression changes between high- and low- fat diet fed mice and identified sexually dimorphic patterns, as well as genes regulating ion balance and chemoreception (39). Similarly, sex-specific expression patterns are also found in mice with maternal overnutrition, although only a limited number of genes were found to be consistently affected (22).

However, gene expression is not the only molecular phenotype that is affected by maternal nutrition. DNA methylation patterns can also respond to environmental perturbations, and mark chromatin changes that affect transcription. To address these epigenetic responses, a recent study of infant growth restriction in humans (40) reported that the methylation patterns of ~27,000 loci in placentas from pregnancies yielding IUGR were found to be significantly different from those of appropriate for gestational age (AGA) placentas. DNA methylation is also known to play a key role in the regulation of placental imprinted genes. The expression of imprinted genes within the placenta affects the allocation of resources between a mother and her offspring (17, 28, 46). It is thought that maternally imprinted genes tend to limit fetal growth, while paternally imprinted genes tend to favor fetal growth (15). Thus imprinted genes in the placenta may have a direct effect on fetal development by affecting nutrient flow and fetal size (19, 41). Furthermore, as one allele in imprinted genes is already functionally silenced, an epigenetic alteration of the other allele can significantly affect transcription. In a previous study of mice reared on high fat diet, several imprinted genes were shown to have sex- and diet-specific changes of expression and DNA methylation (23).

To measure the effect of the intrauterine environment on the placenta, we have previously assessed trans-placental nutrient transport in the wild type and null mouse models, specifically the glucose transporter isoform-3 (GLUT3; placenta)-null heterozygous$^{+/-}$ mutation-carrying mice (25). We found that when the glucose transporter Glut3, which is expressed in the placenta, is deleted on one allele it leads to reduced transplacental glucose transport and sexually dimorphic adiposity with insulin resistance in the adult offspring.

Based on this accumulation of information, we hypothesized that maternal calorie restriction that results in intra-uterine growth restriction would differentially affect placental gene expression and DNA methylation in a sex-specific manner. To test this hypothesis, we employed a murine model of IUGR, and measured both changes in gene expression and DNA methylation. This model differs from previous mouse models of maternal diet effects, which primarily focused on overnutrition. Instead we model the effect of caloric restriction, which mimics the human IUGR phenotype of a low birth weight offspring encountered world-wide that are predisposed to metabolic disorders (24, 27, 30).

We identified differentially expressed genes from RNA-seq data, and examined their associated pathways that are affected by late gestation maternal caloric restriction. Subsequently, we asked whether the DNA methylation profiles are also altered by maternal caloric restriction. To answer this question, we examined genome wide DNA methylation in placentas using reduced representation bisulfite sequencing (RRBS) (42, 52). We observed a decrease in the overall methylation of caloric restricted placentas compared to those exposed to normal diets. We performed a genome wide scan of differentially methylated genes between calorie restricted (CR) versus control (CON) groups and identified chromosomal hotspots for methylation changes that are affected by maternal caloric restriction. We also found an enrichment of known imprinted genes among the differentially methylated genes and identified several differentially methylated microRNAs.

Results

In order to profile transcription and DNA methylation in mouse placentas, we employed our established model of maternal caloric restriction in mice and compared the expression and methylation state of calorically restricted placentas to those of normal control placentas (see Materials and Methods, and Supplementary Information for the details of our mouse models). In total we collected 10 placentas for genome wide DNA methylation profiling (RRBS), and another 10 placentas for expression analysis (RNA-seq). Each placenta arose from separate pregnancies. Equal numbers of samples were collected in each group, i.e., 5 from calorically restricted mice (CR), and 5 placentas from control (see Supplementary Information for sex determination of mice, and Table S1A/S1B for the number of samples in different diet and sex groups.). The placentas are collected after 10 days of caloric

restriction and therefore we hypothesize that the changes in expression and methylation between CR and CON are associated with this altered environment. From previous data we know that CR mice tend to develop increased fat mass and glucose intolerance compared to control mice (30).

The RNA and genomic DNA from placenta samples were extracted for RNA-seq and reduced representation bisulfite library (RRBS) library preparation, followed by massively parallel sequencing with illumina HiSeq 2000 sequencers. The resulting RNA-seq reads were mapped to mouse reference genome (mm9) using Tophat (55) and the differential expression was calculated using DEseq (2) (see Supplementary file 1 for table of expression level per gene). The RRBS reads were mapped using BS Seeker (12) to generate DNA methylation profiles at single base resolution with approximately 50X coverage per strand (see Materials and Methods for the RNA-seq library generation and data processing, RRBS protocols, mapping, and the estimation of methylation levels per cytosine). We compared gene expression and DNA methylation profiles between CR and CON. The differentially expressed genes are defined as those with log 2 ratio greater than 0.2. For differential methylation, the statistical significance is controlled by false discovery rate at <5%, which was estimated by generating synthetic reads from an empirically guided null model in which CR and control samples have the same methylation rates (See Methods for the details of computing false discovery rate).

Maternal caloric restriction resulted in differentially expressed pathways

We began by identifying differential expression between CR and CON (Figure 1A), in which we observed sets of genes that are differentially regulated due to maternal diet. The comparison between sex (Figure S1) shows fewer changes, suggesting that the effect due to maternal diet is stronger than that of gender. Alpha fetoprotein is a protein produced by the liver which changes during pregnancy with growth restriction and other fetal congenital malformations such as neural tube defects, omphalocele and liver defects (49). It is also a clinical marker for IUGR. We found that in our mouse model that this was the most significantly differentially expressed gene based on counts (RPKM), with the affected group showing higher levels than the control, validating our mouse model by reproducing human clinical data. However, this gene also had strong sex-specific effect within females but not in males; females CR showed higher levels of expression and methylation than female CON.

We next searched for gene groups that are enriched in differentially expressed genes, and found several associated with maternal calorie restriction (see Table 1 for selected pathways). Among these were pregnancy specific glycoproteins and lipid-handling proteins. We found that 13 of the 16 pregnancy specific glycoproteins sequenced were down-regulated in CR samples (p-value <0.0001). Pregnancy specific glycoproteins are postulated to have an immunomodulatory role in protecting the fetal allograft, as well as a role in promoting maternal angiogenesis to

202 support the fetus. Lower levels of pregnancy specific glycoproteins have been
203 associated with IUGR, fetal hypoxia and threatened abortion, thus providing a link to
204 the CR associated IUGR phenotype (58, 59). Among the 21 apolipoproteins
205 sequenced, eight were up-regulated in the CR condition, with the remaining 13
206 expressed equally in both conditions (enrichment test: p-value <0.0001). Similarly,
207 two of the five fatty acid-binding proteins (FABPs) were up-regulated in the CR
208 condition, with the remaining three equally expressed (p-value =0.03). This up-
209 regulation likely represents an attempt to increase the nutritional uptake of the
210 calorie-restricted fetus. Indeed, placental expression of some of these
211 apolipoproteins and one or both of the FABPs has been linked to mother-fetus lipid
212 transfer (38, 48). This compensatory response may represent an attempt to
213 maintain the nutrient equipoise and thus represent one mechanism for the
214 increased incidence of adult disease in malnourished fetuses. The FABPs and several
215 of the apolipoproteins involved have been implicated with cardiovascular and
216 metabolic disease in adults, and elevated fetal blood levels of one, ApoB, have
217 already been associated with IUGR and adult atherosclerosis (11, 21, 45).

218 *DNA methylation changes and gender differences*

219

220 We next compared the global DNA methylation levels across our samples (see Table
221 S2A/B for individual samples). The average methylation levels are calculated at
222 1,195,334 cytosines for which we have methylation data across all samples. We
223 observed that the maternal caloric restricted group is less methylated than the
224 control diet mice (p=0.018, T-test, Figure 1A, Table S2C). The average Δ methylation
225 level is approximately 2%. The histogram of Δ methylation levels also shows more
226 sites are less methylated in CR than in CON (Figure 1B). These differences were
227 observed across the genome where particular regions appear to be more
228 differentially methylated (Figure 1C). Furthermore, we found that there is a more
229 significant level of demethylation in male than female mice following caloric
230 restriction (p<2e-16, Kolmogorov-Smirnov test, see Figure S1 for histograms of Δ
231 methylation levels by sex). The methylation difference due to maternal diet in
232 males is 67% more than that in females.

233

234 We next investigated whether differential methylation is associated with specific
235 genomic features, such as coding genes, exons, CpG islands and repetitive sequences
236 and observed no distinct patterns between these, suggesting that the change of
237 methylation is generally non-specific (Figure S2). These methylation patterns in
238 mouse placentas are similar to those in mouse embryos, except the overall
239 methylation level is lower (18). However, we do observe that intrauterine growth
240 restriction (IUGR) dramatically affects the methylation of specific loci. For example,
241 a detailed view of chromosome 13 (Fig 1D) shows that certain megabase-sized
242 regions are hypermethylated in CR compared to CON, with gender specific
243 differences. The genes within this region are found to be associated with genetic
244 disorders, skeletal and muscular disorders, and developmental disorders (Table S3).
245 Lastly, we compared male and female placentas independent of diet, to identify

246 general sex-specific methylation differences in placentas (see Supplementary
247 Information).
248

249 *Differentially methylated genes are clustered across the genome*
250
251 Given the observed global changes of methylation profiles in CR, we searched for
252 hotspots of differential methylation that are affected by maternal diet. RRBS
253 fragments are enriched for CG rich regions and CpG islands, and hence are also
254 enriched for *cis*-regulatory sites. Thus changes in their methylation could either
255 cause, or be associated with changes in transcriptional regulation. As expected, we
256 find that the distribution of methylation levels in CR fragments tends to be slightly
257 lower than CON fragments in both genders ($p<2.2e-16$, Kolmogorov-Smirnov test,
258 see Figure S3). Within these testable fragments we identified 477 differentially
259 methylated regions (DMR, False Discovery Rate <5%) of significance between CR
260 and CON (for the detailed statistical procedure see Materials and Methods). These
261 DMRs are depleted from promoter regions (Figure 2A). Instead, intergenic regions
262 are enriched with DMRs (Figure 2B), which agrees with a recent finding that distal
263 regulatory regions, where transcriptional regulatory enhancers are often located,
264 show altered methylation status (53). Our DMRs are proximal to 297 genes. Of
265 these, 131 genes are hypermethylated in CR samples, and 168 are hypomethylated
266 (Table S4, see Supplementary file 2 for list of DMR and genes). Although the
267 differentially methylated genes are generally spread across the genome, we did find
268 some clusters within chromosomes (Supplementary file 3). Figure 2C and 2D show
269 the distribution of DMRs in the genome and in chromosome 4 where some of these
270 clusters reside.
271
272 As a validation of the RRBS-predicted DMRs, we performed traditional bisulfite
273 sequencing (see (10) for method and Table S5 for primers) on three DMRs that are
274 flagged to be differentially methylated between male CR and male CON (Figures 3
275 and S4). Using this approach we were able to validate two of the three loci, which
276 showed significant changes in the validation data. Figure 3 shows one of the DMRs
277 with a significant change in methylation level in both RRBS and the traditional
278 bisulfite sequencing (32% and 13% respectively). In this locus we find several sites
279 that have significant differential methylation between CR and CON, as shown by the
280 red stars. Despite the fact that one of the loci was not significantly differentially
281 methylated in the validation data, all three DMRs were consistent with respect to
282 the direction of methylation differences.
283
284 To investigate if imprinted genes in placentas are more susceptible to methylation
285 changes in response to diet, we compared our list of differentially methylated genes,
286 between CR and CON and between genders, to 113 known imprinted genes
287 (Supplementary file 4) (43). We found that differentially methylated genes are
288 enriched among the 81 known imprinted genes that are covered by our data; 9 (*Igf2,*
289 *Inpp5f, Dlk1, Gnas, Usp29, Wt1, Kcnk9, Grb10, Cdkn1c,*) show differential methylation
290 in CR with or without sex preference, and 7 between genders (*Nnat, Mest, Blcap,*

291 *Peg13, Snrpn, Grb10, Gnas)* (p-values<0.09, using the hypergeometric test of
292 enrichment). This enrichment of imprinted genes suggests that the methylation of
293 these genes may be more sensitive to changes in the environment.
294
295 For example*, Inpp5f* is an imprinted gene that regulates cardiac hypertrophic
296 responsiveness. It has been reported to be paternally expressed and maternally
297 methylated (13). We identified a CpG island within the gene that was significantly
298 hyper methylated in CR (see Fig 4B). Another imprinted gene *Igf2* serves as a fetal
299 growth factor which associates with fetal growth(14). In a study of Igf2P0 (placenta
300 specific knock out) mouse, a decrease in system A amino acid transport across the
301 placenta was reported with fetal growth restriction (50). In our data we observed
302 altered methylation patterns in exon 3 of *Igf2* corresponding to a hyper methylated
303 state in CR samples. These findings are consistent with previous reports in IUGR
304 that imprinted genes in placentas are susceptible to epigenetic changes (46).
305

306 *Differential methylation is associated with genes related to cardiovascular,*
307 *metabolic, and neurological diseases*
308
309 We performed a functional analysis of the differentially methylated genes using the
310 DAVID Bioinformatics Resources 6.7 (29) and the Ingenuity Pathway Analysis tool
311 (1). We found that differentially methylated genes in CR are enriched for functional
312 categories such as transcriptional regulation, learning, cytoplasmic vesicle, cell
313 morphogenesis involved in neuron differentiation, lipid binding, regulation of
314 neuron apoptosis, behavior, and fatty acid metabolic process (Table S6). In the
315 network analysis, we found that the major networks are enriched with functions in
316 embryonic development, nervous system development and cardiovascular system
317 development and function (Table 2). The associated disorders include
318 cardiovascular disease (e.g., heart disease, vascular disease), neurological disease
319 (e.g., bipolar, Parkinson's, Alzheimer's diseases), and metabolic disorders (e.g,
320 Crohn's disease, non-insulin dependent diabetes mellitus). Although there may not
321 be direct links between the differential methylation we observe and these diseases,
322 it is proposed that alterations to placental pathways could potentially be similar to
323 those found within the fetus and thus link IUGR to the above late onset disorders
324 (40). Figure S5 (network view) shows a major network including 21 differentially
325 methylated genes that are enriched with functions in cardiovascular system
326 development and function, cellular movement and embryonic development.
327

328 *Sex Specific Effects on maternal caloric restriction*
329
330 We identified 667 differentially methylated genes (FDR<=4.03%) that are
331 significantly differentially methylated between CR and CON in a sex specific manner
332 (see Materials and Methods). Of these genes, 380 genes are hypermethylated in
333 male CR versus male CON as opposed to the female CR versus female CON, and 309

genes show inversely hypermethylation in female CR versus female CON (Table S4, see Supplementary file 2 for list of DMR and genes). This large number of genes is distributed throughout the genome (Figure S6), suggesting the changes of methylation in response to maternal diet have a strong sex specific component. In the functional analysis, we found that these differentially methylated genes are enriched with functions in embryonic morphogenesis, metabolic processes (Table S6), and with the networks of cellular development, nucleic acid metabolism, and auditory and vestibular system development (Table 2). Specifically, the genes that are hyper methylated in female CR are enriched in the network of lipid metabolism, nerve system development and function, and developmental disorders, whereas those hypermethylated in male CR are enriched in networks of cell and organ morphology. Placentas are functional during a critical developmental window in which both the gametes and the sex organs are determined. The functional categories we identified contain key genes that are possibly under epigenetic control within the fetus and affect these processes.

Prostaglandin Receptor and Glucose Transporter

To further examine the relationship between DNA methylation and transcription in the differentially methylated genes, we performed qRT-PCR (see Supplementary Information for RNA preparation and qRT-PCR) on the prostaglandin E receptor 1 (*ptger1*), which we observed to be less methylated in CR at a CpG island in the second exon (Figure 4A). Interestingly, the change of methylation is significantly greater in females than in males. An increased expression level is observed in CR (p-value=0.012, t-test, 26 biological replicates, see Figure 5A), suggesting that the change of methylation at *ptger1* is associated with its transcription. However, only the female CR group shows a significant change in expression, which is consistent with the female specific methylation change. *Ptger1* is a receptor of Prostagandin E2 (PGE2), which is a vasodilator that acts to lower blood pressure and also acts to induce labor. *Ptger1* with its function of regulating blood pressure has also been associated with diabetes, preeclampsia, and premature birth; all three conditions can be associated with IUGR and have long term fetal programming implications. Ptger1 is also known to mediate hypertension resulting in end organ damage (4).

A second gene of interest is the glucose transporter isoform 3 (Glut3). We have previously shown that maternal CR in mice led to a decrease in placental Glut3 protein expression along with a functional decrease in trans-placental glucose transport (24, 26). Furthermore, using candidate gene specific methylation sensitive PCR we detected hypermethylation of this gene in placentas exposed to CR (unpublished data under review). The CpGs within a stretch that extended from -805 to 922 bp 5' to the transcription start site were specifically hypermethylated. This hypermethylation was associated with a decrease in placental Glut3 expression. In our present investigation, we explored this further using our genome-wide data and confirmed that the Glut3 gene, situated on the negative strand of

379 chromosome 6, is hypermethylated in CR versus CON (Fig S7). Specifically +717 to
380 +1040 bp, 5' to the TSS was hypermethylated (p=0.008). Thus in the case of a gene
381 that is critically important for transplacental glucose transport and embryonic
382 survival (26), DNA methylation in CR was associated with changes in gene
383 expression and its ultimate function.
384

385 *Differentially methylated microRNAs target metabolic genes*
386
387 MicroRNAs affect post-transcriptional regulation of genes, typically regulating the
388 transcription and translation of many target genes. MicroRNAs have also been
389 shown to play a role in epigenetic inheritance in mice (57). We found within our list
390 of differentially methylated genes 19 microRNAs (Table S7). miR-149 is only 65 bp
391 in length and is encoded in one hypermethyated fragment in CR versus CON (Figure
392 4C). RT-qPCR (see Supplementary Information for qRT-PCR of miR-149) shows that
393 this gene is differentially expressed in CR versus CON in placentas (p=0.026, t-test,
394 20 biological replicates, see Figure 5B); suggesting that the difference of
395 methylation may be associated with its expression. Gene ontology analysis of its
396 target genes finds that these are enriched for functions associated with embryonic
397 development and associated with cardiovascular and metabolic diseases. One of its
398 target genes is the system L amino acid transporter isoform 2 (LAT2), which in
399 females is hypermethylated in CR versus CON but not in males. The expression of
400 placental LAT2 however shows no expression change in response to maternal CR
401 but a decline in protein abundance, supporting the notion that in this case the
402 miRNA regulates protein translation (unpublished data under review). The decrease
403 in LAT2 mediates diminished transplacental leucine transport in CR. Thus in CR,
404 hypermethylation of the miR-149 gene body leads to increased miR-149 gene
405 expression which is associated with decreased LAT2 protein concentrations.
406
407

408 *The association between changes of DNA methylation and gene expression*
409
410 The global correlation between the changes of DNA methylation and gene
411 expression is weak (Pearson correlation <5%). However, we found that
412 differentially methylated genes had a greater variation in gene expression
413 (measured via RPKM) compared to all genes (Figure 6A/B, Figure S10), suggesting
414 that changes in DNA methylation tend to increase the variability of gene expression.
415 To further study the effect of methylation changes in transcription changes, we plot
416 methylation levels in promoters and gene bodies ranked by their changes in gene
417 expression levels (Figure 6C/D, Figure S11). The result shows that in our data gene
418 bodies have a stronger association with expression than promoters. We find that
419 genes whose expression increases in CR vs. CON tend to lose methylation within the
420 gene body, but are unaffected in their promoters. This suggests a subtle coupling
421 between the rate of transcription and methylation, suggesting that the latter is
422 dynamically regulated by the transcriptional machinery.

Discussion

In this study, we generated placental genome wide DNA methylation and transcriptional profiles in CR and CON pregnant mice. We identified differentially regulated pathways associated with IUGR, including a significant change in alpha-fetoprotein as well as pregnancy specific glycoproteins. We also observed a mild decrease of global methylation levels in CR. We find that CR samples consistently have lower methylation levels throughout the genome. This results is consistent with previous reports from specific loci in rats that showed that prenatal nutritional constraints result in hypomethylation (33, 34), and that the reduced expression of DNMT1 is likely involved in this impaired methylation. Furthermore these studies examine the connection between hypomethylation and a wide range of developmental and metabolic processes (6, 32).

We identified 297 genes that are significantly differentially methylated due to maternal caloric restriction. These genes are clustered within chromosomes, supporting the notion that while maternal diet affects global DNA methylation levels of the placenta, certain regions appear to be more susceptible than others. These placental mechanisms that are mediated by epigenetic adaptation may promote fetal survival at the expense of achieving optimal energy balance and growth. While surviving the adverse in-utero environment, some of these perturbations in gene methylation may predispose the offspring for adult-type chronic diseases. Thus, specific genes that are epigenetically regulated could serve as placental biomarkers for predicting the potential of developing the disease phenotype in the adult, which could be clinically important for diagnosing and predicting the outcome of low birth weight babies.

We also found that known imprinted genes are significantly enriched in our lists of differentially methylated genes between CR and CON, and between genders. This suggests that imprinted genes in placentas are particularly sensitive to environmental changes. This observation supports previous findings that these genes are often critical for establishing the growth and size of the developing fetus, and are under different adaptive pressures depending on whether they are maternally or paternally imprinted.

Ptger1 was found to be one of the most significant sex specific differentially methylated genes in CR versus CON. This raises a possibility that dysregulation of DNA methylation of the *Ptger1* gene in females may underlie the mechanism of preterm birth in maternal undernutrition. It has been clinically and experimentally shown that preterm birth rate increases in the cohort conceived during famine and animals fertilized under caloric restriction (8, 20, 35, 36, 51, 54). *Ptger1* mediates the effect of prostaglandin E2 (PGE2), an uterotonic agent that is clinically used for

466 prevention of postpartum hemorrhage as well as induction of abortion.
467 Upregulation of *Ptger1* in the female CR group in our study increases the effect of
468 PGE2, which may lead to the contraction of the uterus and preterm delivery. These
469 functional consequences need to be further investigated in our murine model of
470 maternal CR in the future.
471
472 An unexpected result in our data is the enrichment of differentially methylated
473 genes that are associated with cardiovascular disease. This observation is consistent
474 with the previous publications by us and others demonstrating that extra-
475 embryonic tissues display latent cardiogenic potential: a population of yolk sac cells
476 show contractile phenotype in *ex vivo* culture (44) or by genetic manipulation (56),
477 and placental cells may contribute to the maternal heart during peripartum
478 cardiomyopathy (31). Thus, our current data might suggest that this latent
479 cardiogenic potential is sensitive to the nutrition status.
480
481 Fetal malnutrition is linked to the risk of adult cardiovascular diseases including
482 coronary heart disease (47). This may be due to the placental malfunction, as
483 reconstitution of the placenta restores heart development in an experimental
484 setting (3). Alternatively, our data raises the possibility that the methylation status
485 of the cardiovascular genes in the placenta is sensitive to the nutritional state in
486 other tissues including the heart. The direct impact of malnutrition on DNA
487 methylation of cardiovascular tissues remains to be elucidated in the future.
488
489 MicroRNAs have been implicated in epigenetic regulation by post-transcriptionally
490 altering transcripts (16). Our finding of differential methylation of certain placental
491 miRNAs by maternal CR is novel. Particularly the observation that the
492 hypermethylation of the miR-149 gene body is associated with enhanced miR-149
493 gene expression. While LAT2 was known to be a target of this miRNA, previous
494 investigations by us have demonstrated that maternal CR led to no change in
495 placental LAT2 mRNA. However, measurement of the LAT2 protein revealed that it
496 has reduced concentrations in response to CR (24). Thus it appears that maternal
497 CR may affect initiation of LAT2 protein translation via activation of miR-149
498 expression. LAT2 is a system L amino acid transporter that mediates transplacental
499 branched chain amino acid transfer (e.g. leucine, isoleucine). In the IUGR fetus, there
500 is a perceptible decrease in circulating branched chain amino acids, perhaps related
501 to a diminution of transplacental transfer. Combining the information on placental
502 Glut3 and LAT2 in CR, it appears that while Glut3 DNA hypermethylation
503 transcriptionally affects its gene expression, hypermethylation of miR-149 post-
504 transcriptionally may affect the protein translation of LAT2. Both of these genes
505 mediate transplacental nutrient transport and are critically important in fueling
506 fetal energy metabolism and growth. In CR, diminished concentrations of both these
507 proteins results in reduced materno-fetal glucose and leucine transport, thereby
508 contributing to diminished fetal growth and its associated consequences (24).
509
510 Our study investigates altered transcription and methylation in placentas. We
511 identified the enriched functions of differentially expressed or methylated genes as

512 possible phenotypes. Our results strongly support the notion that the expression
513 and methylation state of the placenta is sensitive to the intrauterine environment,
514 and it is likely that these changes have profound effects on fetal development.
515 Measuring genes in the placenta is important to identify potential markers of IUGR
516 as well as suggesting new biochemical mechanisms that could affect fetal
517 development.

518 Materials and Methods

519 *Mouse placenta samples*

520

521 Animals: C57/BL6 mice were housed in 12:12 hour light dark cycles with ad libitum
522 access to a standard rodent chow diet (Harlan Teklad 7013) and water. At eight
523 weeks of age, male and female mice were mated overnight and the presence of a
524 vaginal plug in the female was designated as gestational day 1. Pregnant females
525 were transferred to individual cages and reared on the same chow diet ad libitum.
526 At gestational day 10, the pregnant mice were arbitrarily divided into two groups,
527 one group which served as the control (CON) continued to receive ad libitum chow
528 diet. The second group was subjected to caloric restriction (CR) by providing 50%
529 (wt) of their daily intake until gestational day 19. This particular time of late
530 gestation was used because the impact of placental function dramatically affects
531 fetal growth at this time. Late gestation is the time period during which placental gene
532 expression significantly affects fetal growth patterns. It has been shown that when
533 glucose transport across the placenta is affected, fetal growth is diminished during
534 late gestation including day 19 (25, 26). At this time, the animal was euthanized by
535 receiving 100 mg/kg of Phenobarbital i.p. The placentas were separated from the
536 respective fetuses and collected. After accurate weighing of the placentas in a
537 Mettler AB104 precision balance (0.01 mg sensitivity, see Table S8) they were snap
538 frozen immediately and stored at -80°C until further analyses. This study protocol
539 (24) was approved by the Animal Research Committee of the University of
540 California Los Angeles (UCLA) in accordance with the guidelines set by the National
541 Institutes of Health.
542

543 *RNA-seq library generation and data processing*

544

545 After RNA extraction (see Supplementary Information), total RNA was quantified
546 using Qubit RNA assay and 1000 ng were used as starting material for each sample.
547 The library preparation was performed using the Illumina TruSeq RNA Sample
548 Preparation kit using manufacturer's instructions. Libraries were run using 50-bp
549 single-end reads on the HiSeq 2000 System (Illumina). The reads are mapped using
550 Tophat (55) allowing up to 2 mismatches and only unique alignments are kept. The
551 quality of alignments are checked using FastQC. The resulted alignment file are
552 processed through HTSeq program along with annotation file to create gene matrix,

553 as the input for downstream analysis. The differential expression is calculated using
554 DESeq (2) to generate Reads Per Kilobase per Million mapped reads (RPKM) per
555 gene (Supplementary file 1).
556

557 *Reduced representation bisulfite sequencing*
558
559 Genomic DNA from our mice placentas was extracted for making RRBS libraries
560 following the standard RRBS protocol (42). The genome was digested with the MspI
561 enzyme, a methylation-insensitive restriction enzyme. Fragments from 100 to 200
562 bases were selected as these are enriched for CpG rich regions, such as CpG islands,
563 promoter regions, and enhancer elements. In total we selected 500K fragments for
564 sequencing. These MspI-digested samples were ligated with Illumina adaptors, and
565 size selected, denatured and treated with sodium bisulfite to reveal their
566 methylation status. These libraries were sequenced using Solexa sequencing
567 technology (illumna Hiseq 2000 sequencers). The reads were aligned to the
568 reference genome (mouse mm9) using the modified bisulfite aligner, BS Seeker, to
569 keep track of the fragment that each alignment was uniquely mapped to. To
570 generate genome wide DNA methylation profiles, we calculate methylation level for
571 each covered cytosine on the genome. As bisulfite treatment converted
572 unmethylated cytosines (Cs) to thymines (Ts), we estimate the methylation level at
573 each cytosine by #C/(#C+#T), where #C is the number of methylated reads and #T
574 is the number of unmethylated reads. The methylation level per cytosine serves as
575 an estimate of the percentage of cells that are methylated at this cytiosine. In this
576 study we only include cytosines that are covered by at least four reads for the
577 analyisis. The resulting methylation profile per sample covered about 1.4M CpG
578 sites. These profiles can be seen through our genome browser at http://genomes-
579 prepub8.mcdb.ucla.edu (`login:` prepub8
580 `password:` `VnghRZWY`) and can be downloaded from LINK (available upon
581 published).
582

583 *Identifying differentially methylated regions (DMR) and the associated*
584 *genes*
585
586 We first searched for DMR that show significant differential methylation. Genes that
587 are close to these DMR are considered differentially methylated.
588
589 For each CG site we calculated a t-score from the T-test of mean difference between
590 the two groups of comparison, then select sites with |t-score| >=1.5 (approx. top
591 10%) as markers of differential methylation. If two markers are within 80bp (in our
592 data median distance =74bp) then the region between them is deemed candidate
593 DMR. For each candidate DMR we then calculate a z score of the average t score
594 from all CG sites within the region, as a measure of the differential methylation
595 within this candidate DMR. When the |z-score| is greater than a threshold and the

596 mean methylation levels in the two groups differ by at least 15%, this region is
597 considered as differentially methylated (DMR). The selection of z score threshold is
598 based the false discovery rate estimated as described below. In our analysis,
599 hypermethylation in CR group, or in female group, has positive z scores. Finally, if
600 the genes overlap with any of these DMRs, or if their transcription start sites are
601 within 5Kbp of the DMR, these genes are deemed differentially methylated. In total,
602 we identified 297 genes that are differentially methylated between CR and CON, and
603 527 between male and female.
604
605 The DMR of CR vs. CON with sex effect was based on the comparison of two t-tests
606 (male comparison: male CR vs. male CON, and female comparison: female CR vs.
607 female CON). The t-score here is estimated by (t-score from female) - (t-score from
608 male), and the same approach is used for calculating Δ m.
609

610 *Estimating false discovery rate (FDR)*

611
612 To assess the false discovery rate for our DMRs, we constructed 10 simulated
613 methylomes, with the same read coverage per site as the real samples. For each CG
614 site in each simulated sample, we then simulated the reads (C if methylated, or T if
615 unmethylated) based on the average methylation level (Pm) from all real samples at
616 this CG site. The number of methylated reads (Cs) at a site of coverage n is a random
617 sample from the binomial distribution B(n,Pm). We repeat our simulation of reads
618 throughout the genome for all 10 samples. The resulting samples have the sample
619 average methylation levels as the real sample, since the reads were simulated from
620 the binomial distribution with the same average methylation levels as in the real
621 samples, so the differences in methylation patterns across genes, repeats,
622 promoters, etc are preserved. The simulated data also has the same coverage as the
623 real samples so the statistical power is not affected. The simulated methylomes
624 should have no difference in methylation levels between the two comparison groups
625 (i.e., no DMR), since they are all selected using the same methylation frequency. Any
626 DMR (and the DMR associated genes) identified from these simulated samples are
627 thus considered false positives. Finally, for each comparison (e.g. CR vs. CON) we
628 repeated the whole procedure to detect the DMR on simulated samples.The
629 resulting false discovery rates are less than 5% in all comparisons (See Table S9 for
630 FDR).
631
632 To identify hotspots of differential methylation (i.e., genomic regions that are
633 significantly clustered with differentially methylated genes) we tested the
634 enrichment of differentially methylated genes within non-overlapping windows of
635 3Mb in the genome using the hypergeometric distribution. The p-value cutoffs are
636 selected such that the false discovery rate (estimated by R module p.adjust using
637 Benjamin's method (5)) is less than 5% ($p<=0.002$ for the comparison between CR
638 vs. CON, $p<=0.0007$ for diet response with sex effect, $p<=0.003$ for sex
639 comparisons).
640

Acknowledgments

The authors thank Weihong Yan for the data visualization on genome browser. This work was supported by the National Institutes of Health (HD-46979, HD-33997, HD-25024 and HD-41320) to SUD, and R01 GM095656-01A1 to MP. S.F. is Special Fellow of the Leukemia & Lymphoma Society.

1. Ingenuity Pathway Analysis software. Ingenuity Systems, CA, USA.
2. **Anders S, and Huber W**. Differential expression analysis for sequence count data. *Genome Biol* 11: R106, 2010.
3. **Barak Y, Nelson MC, Ong ES, Jones YZ, Ruiz-Lozano P, Chien KR, Koder A, and Evans RM**. PPAR gamma is required for placental, cardiac, and adipose tissue development. *Mol Cell* 4: 585-595, 1999.
4. **Bartlett CS, Boyd KL, Harris RC, Zent R, and Breyer RM**. EP1 disruption attenuates end-organ damage in a mouse model of hypertension. *Hypertension* 60: 1184-1191, 2012.
5. **Benjamini Y, and Hochberg Y**. Controlling the False Discovery Rate - a Practical and Powerful Approach to Multiple Testing. *Journal of the Royal Statistical Society Series B-Methodological* 57: 289-300, 1995.
6. **Bertram C, Trowern AR, Copin N, Jackson AA, and Whorwood CB**. The maternal diet during pregnancy programs altered expression of the glucocorticoid receptor and type 2 11beta-hydroxysteroid dehydrogenase: potential molecular mechanisms underlying the programming of hypertension in utero. *Endocrinology* 142: 2841-2853, 2001.
7. **Bhasin KK, van Nas A, Martin LJ, Davis RC, Devaskar SU, and Lusis AJ**. Maternal low-protein diet or hypercholesterolemia reduces circulating essential amino acids and leads to intrauterine growth restriction. *Diabetes* 58: 559-566, 2009.
8. **Bloomfield FH, Oliver MH, Hawkins P, Campbell M, Phillips DJ, Gluckman PD, Challis JR, and Harding JE**. A periconceptional nutritional origin for noninfectious preterm birth. *Science* 300: 606, 2003.
9. **Burton GJ, Jauniaux E, and Charnock-Jones DS**. The influence of the intrauterine environment on human placental development. *Int J Dev Biol* 54: 303-312, 2010.
10. **Cao X, and Jacobsen SE**. Locus-specific control of asymmetric and CpNpG methylation by the DRM and CMT3 methyltransferase genes. *Proc Natl Acad Sci U S A* 99 Suppl 4: 16491-16498, 2002.
11. **Chan DC, Barrett HP, and Watts GF**. Dyslipidemia in visceral obesity: mechanisms, implications, and therapy. *Am J Cardiovasc Drugs* 4: 227-246, 2004.
12. **Chen PY, Cokus SJ, and Pellegrini M**. BS Seeker: precise mapping for bisulfite sequencing. *BMC Bioinformatics* 11: 203, 2010.
13. **Choi JD, Underkoffler LA, Wood AJ, Collins JN, Williams PT, Golden JA, Schuster EF, Loomes KM, and Oakey RJ**. A novel variant of Inpp5f is imprinted in brain, and its expression is correlated with differential methylation of an internal CpG island. *Molecular and Cellular Biology* 25: 5514-5522, 2005.

686 14. **Constancia M, Angiolini E, Sandovici I, Smith P, Smith R, Kelsey G, Dean**
687 **W, Ferguson-Smith A, Sibley CP, Reik W, and Fowden A**. Adaptation of nutrient
688 supply to fetal demand in the mouse involves interaction between the Igf2 gene and
689 placental transporter systems. *Proc Natl Acad Sci U S A* 102: 19219-19224, 2005.
690 15. **Constancia M, Kelsey G, and Reik W**. Resourceful imprinting. *Nature* 432:
691 53-57, 2004.
692 16. **Devaskar SU, and Raychaudhuri S**. Epigenetics--a science of heritable
693 biological adaptation. *Pediatr Res* 61: 1R-4R, 2007.
694 17. **El-Maarri O, Buiting K, Peery EG, Kroisel PM, Balaban B, Wagner K,**
695 **Urman B, Heyd J, Lich C, Brannan CI, Walter J, and Horsthemke B**. Maternal
696 methylation imprints on human chromosome 15 are established during or after
697 fertilization. *Nat Genet* 27: 341-344, 2001.
698 18. **Feng S, Cokus SJ, Zhang X, Chen PY, Bostick M, Goll MG, Hetzel J, Jain J,**
699 **Strauss SH, Halpern ME, Ukomadu C, Sadler KC, Pradhan S, Pellegrini M, and**
700 **Jacobsen SE**. Conservation and divergence of methylation patterning in plants and
701 animals. *Proc Natl Acad Sci U S A* 107: 8689-8694, 2010.
702 19. **Fowden AL, Sibley C, Reik W, and Constancia M**. Imprinted genes,
703 placental development and fetal growth. *Horm Res* 65 Suppl 3: 50-58, 2006.
704 20. **Fowden AL, and Silver M**. The effect of the nutritional state on uterine
705 prostaglandin F metabolite concentrations in the pregnant ewe during late
706 gestation. *Q J Exp Physiol* 68: 337-349, 1983.
707 21. **Furuhashi M, and Hotamisligil GS**. Fatty acid-binding proteins: role in
708 metabolic diseases and potential as drug targets. *Nat Rev Drug Discov* 7: 489-503,
709 2008.
710 22. **Gabory A, Ferry L, Fajardy I, Jouneau L, Gothie JD, Vige A, Fleur C,**
711 **Mayeur S, Gallou-Kabani C, Gross MS, Attig L, Vambergue A, Lesage J, Reusens**
712 **B, Vieau D, Remacle C, Jais JP, and Junien C**. Maternal diets trigger sex-specific
713 divergent trajectories of gene expression and epigenetic systems in mouse placenta.
714 *PLoS One* 7: e47986, 2012.
715 23. **Gallou-Kabani C, Gabory A, Tost J, Karimi M, Mayeur S, Lesage J, Boudadi**
716 **E, Gross MS, Taurelle J, Vige A, Breton C, Reusens B, Remacle C, Vieau D,**
717 **Ekstrom TJ, Jais JP, and Junien C**. Sex- and diet-specific changes of imprinted gene
718 expression and DNA methylation in mouse placenta under a high-fat diet. *PLoS One*
719 5: e14398, 2010.
720 24. **Ganguly A, Collis L, and Devaskar SU**. Placental glucose and amino acid
721 transport in calorie-restricted wild-type and Glut3 null heterozygous mice.
722 *Endocrinology* 153: 3995-4007, 2012.
723 25. **Ganguly A, and Devaskar SU**. Glucose transporter isoform-3-null
724 heterozygous mutation causes sexually dimorphic adiposity with insulin resistance.
725 *Am J Physiol Endocrinol Metab* 294: E1144-1151, 2008.
726 26. **Ganguly A, McKnight RA, Raychaudhuri S, Shin BC, Ma Z, Moley K, and**
727 **Devaskar SU**. Glucose transporter isoform-3 mutations cause early pregnancy loss
728 and fetal growth restriction. *Am J Physiol Endocrinol Metab* 292: E1241-1255, 2007.
729 27. **Garg M, Thamotharan M, Pan G, Lee PW, and Devaskar SU**. Early
730 exposure of the pregestational intrauterine and postnatal growth-restricted female

731 offspring to a peroxisome proliferator-activated receptor-{gamma} agonist. *Am J*
732 *Physiol Endocrinol Metab* 298: E489-498, 2010.
733 28. **Haig D, and Westoby M**. Parent-Specific Gene-Expression and the Triploid
734 Endosperm. *American Naturalist* 134: 147-155, 1989.
735 29. **Huang da W, Sherman BT, and Lempicki RA**. Systematic and integrative
736 analysis of large gene lists using DAVID bioinformatics resources. *Nat Protoc* 4: 44-
737 57, 2009.
738 30. **Jimenez-Chillaron JC, Isganaitis E, Charalambous M, Gesta S, Pentinat-**
739 **Pelegrin T, Faucette RR, Otis JP, Chow A, Diaz R, Ferguson-Smith A, and Patti**
740 **ME**. Intergenerational transmission of glucose intolerance and obesity by in utero
741 undernutrition in mice. *Diabetes* 58: 460-468, 2009.
742 31. **Kara RJ, Bolli P, Karakikes I, Matsunaga I, Tripodi J, Tanweer O, Altman**
743 **P, Shachter NS, Nakano A, Najfeld V, and Chaudhry HW**. Fetal cells traffic to
744 injured maternal myocardium and undergo cardiac differentiation. *Circ Res* 110: 82-
745 93, 2012.
746 32. **Lillycrop KA, Phillips ES, Jackson AA, Hanson MA, and Burdge GC**. Dietary
747 protein restriction of pregnant rats induces and folic acid supplementation prevents
748 epigenetic modification of hepatic gene expression in the offspring. *J Nutr* 135:
749 1382-1386, 2005.
750 33. **Lillycrop KA, Phillips ES, Torrens C, Hanson MA, Jackson AA, and Burdge**
751 **GC**. Feeding pregnant rats a protein-restricted diet persistently alters the
752 methylation of specific cytosines in the hepatic PPAR alpha promoter of the
753 offspring. *Br J Nutr* 100: 278-282, 2008.
754 34. **Lillycrop KA, Slater-Jefferies JL, Hanson MA, Godfrey KM, Jackson AA,**
755 **and Burdge GC**. Induction of altered epigenetic regulation of the hepatic
756 glucocorticoid receptor in the offspring of rats fed a protein-restricted diet during
757 pregnancy suggests that reduced DNA methyltransferase-1 expression is involved in
758 impaired DNA methylation and changes in histone modifications. *Br J Nutr* 97: 1064-
759 1073, 2007.
760 35. **Lumey LH, Ravelli AC, Wiessing LG, Koppe JG, Treffers PE, and Stein ZA**.
761 The Dutch famine birth cohort study: design, validation of exposure, and selected
762 characteristics of subjects after 43 years follow-up. *Paediatr Perinat Epidemiol* 7:
763 354-367, 1993.
764 36. **Lumey LH, and Van Poppel FW**. The Dutch famine of 1944-45: mortality
765 and morbidity in past and present generations. *Soc Hist Med* 7: 229-246, 1994.
766 37. **Maccani MA, and Marsit CJ**. Epigenetics in the Placenta. *American Journal of*
767 *Reproductive Immunology* 62: 78-89, 2009.
768 38. **Madsen EM, Lindegaard ML, Andersen CB, Damm P, and Nielsen LB**.
769 Human placenta secretes apolipoprotein B-100-containing lipoproteins. *J Biol Chem*
770 279: 55271-55276, 2004.
771 39. **Mao J, Zhang X, Sieli PT, Falduto MT, Torres KE, and Rosenfeld CS**.
772 Contrasting effects of different maternal diets on sexually dimorphic gene
773 expression in the murine placenta. *Proc Natl Acad Sci U S A* 107: 5557-5562, 2010.
774 40. **Marsit CJ, Banister CE, Koestler DC, Maccani MA, Padbury JF, and**
775 **Houseman EA**. Infant growth restriction is associated with distinct patterns of DNA
776 methylation in human placentas. *Epigenetics* 6: 920-927, 2011.

41. **McMinn J, Wei M, Schupf N, Cusmai J, Johnson EB, Smith AC, Weksberg R, Thaker HM, and Tycko B**. Unbalanced placental expression of imprinted genes in human intrauterine growth restriction. *Placenta* 27: 540-549, 2006.
42. **Meissner A, Gnirke A, Bell GW, Ramsahoye B, Lander ES, and Jaenisch R**. Reduced representation bisulfite sequencing for comparative high-resolution DNA methylation analysis. *Nucleic Acids Res* 33: 5868-5877, 2005.
43. **Morison IM, Paton CJ, and Cleverley SD**. The imprinted gene and parent-of-origin effect database. *Nucleic Acids Res* 29: 275-276, 2001.
44. **Murakami Y, Hirata H, Miyamoto Y, Nagahashi A, Sawa Y, Jakt M, Asahara T, and Kawamata S**. Isolation of cardiac cells from E8.5 yolk sac by ALCAM (CD166) expression. *Mechanisms of development* 124: 830-839, 2007.
45. **Radunovic N, Kuczynski E, Rosen T, Dukanac J, Petkovic S, and Lockwood CJ**. Plasma apolipoprotein A-I and B concentrations in growth-retarded fetuses: a link between low birth weight and adult atherosclerosis. *J Clin Endocrinol Metab* 85: 85-88, 2000.
46. **Reik W, and Walter J**. Genomic imprinting: parental influence on the genome. *Nat Rev Genet* 2: 21-32, 2001.
47. **Roseboom TJ, van der Meulen JH, Osmond C, Barker DJ, Ravelli AC, Schroeder-Tanka JM, van Montfrans GA, Michels RP, and Bleker OP**. Coronary heart disease after prenatal exposure to the Dutch famine, 1944-45. *Heart* 84: 595-598, 2000.
48. **Scifres CM, Chen B, Nelson DM, and Sadovsky Y**. Fatty acid binding protein 4 regulates intracellular lipid accumulation in human trophoblasts. *J Clin Endocrinol Metab* 96: E1083-1091, 2011.
49. **Sebire NJ, Spencer K, Noble PL, Hughes K, and Nicolaides KH**. Maternal serum alpha-fetoprotein in fetal neural tube and abdominal wall defects at 10 to 14 weeks of gestation. *Brit J Obstet Gynaec* 104: 849-851, 1997.
50. **Sferruzzi-Perri AN, Vaughan OR, Coan PM, Suciu MC, Darbyshire R, Constancia M, Burton GJ, and Fowden AL**. Placental-specific Igf2 deficiency alters developmental adaptations to undernutrition in mice. *Endocrinology* 152: 3202-3212, 2011.
51. **Silver M, and Fowden AL**. Uterine prostaglandin F metabolite production in relation to glucose availability in late pregnancy and a possible influence of diet on time of delivery in the mare. *J Reprod Fertil Suppl* 32: 511-519, 1982.
52. **Smith ZD, Gu H, Bock C, Gnirke A, and Meissner A**. High-throughput bisulfite sequencing in mammalian genomes. *Methods* 48: 226-232, 2009.
53. **Stadler MB, Murr R, Burger L, Ivanek R, Lienert F, Scholer A, Wirbelauer C, Oakeley EJ, Gaidatzis D, Tiwari VK, and Schubeler D**. DNA-binding factors shape the mouse methylome at distal regulatory regions. *Nature* 480: 490-495, 2011.
54. **Susser M, and Stein Z**. Timing in prenatal nutrition: a reprise of the Dutch Famine Study. *Nutr Rev* 52: 84-94, 1994.
55. **Trapnell C, Pachter L, and Salzberg SL**. TopHat: discovering splice junctions with RNA-Seq. *Bioinformatics* 25: 1105-1111, 2009.
56. **Van Handel B, Montel-Hagen A, Sasidharan R, Nakano H, Ferrari R, Boogerd CJ, Schredelseker J, Wang Y, Hunter S, Org T, Zhou J, Li X, Pellegrini M,**

823 **Chen JN, Orkin SH, Kurdistani SK, Evans SM, Nakano A, and Mikkola HK**. Scl
824 represses cardiomyogenesis in prospective hemogenic endothelium and
825 endocardium. *Cell* 150: 590-605, 2012.
826 57. **Wagner KD, Wagner N, Ghanbarian H, Grandjean V, Gounon P, Cuzin F,**
827 **and Rassoulzadegan M**. RNA induction and inheritance of epigenetic cardiac
828 hypertrophy in the mouse. *Dev Cell* 14: 962-969, 2008.
829 58. **Wessells J, Wessner D, Parsells R, White K, Finkenzeller D,**
830 **Zimmermann W, and Dveksler G**. Pregnancy specific glycoprotein 18 induces IL-
831 10 expression in murine macrophages. *Eur J Immunol* 30: 1830-1840, 2000.
832 59. **Wynne F, Ball M, McLellan AS, Dockery P, Zimmermann W, and Moore T**.
833 Mouse pregnancy-specific glycoproteins: tissue-specific expression and evidence of
834 association with maternal vasculature. *Reproduction* 131: 721-732, 2006.
835
836

Figure Legends

Figure 1 Comparisons of gene expression and DNA methylation levels in mouse placenta samples. **A.** heatmap of gene expression levels in caloric restricted (CR), and wild type (CON) groups (CR); **B.** Average methylation levels in CR vs. CON; **C.** histogram of Δ methylation levels per CG site between CR and CON; **D.** Log2 ratios of methylation levels between sample groups in genome wide view, and **E.** in chromosome 13.

Figure 2 Distribution of differentially methylated regions (DMR), and genes
A. Meta gene plot of percent DMR of RRBS fragments, **B.** Fold enrichment of DMRs in promoters, exons, introns, and intergenic regions, **C.** distribution of DMRs and the associated genes in a genome wide view, and **D.** in chromosome 4; circles are all candidate regions with the z-scores in y axis, squares are the differentially methylated genes associated to DMR (red circles).

Figure 3: DMR validation using traditional bisulfite sequencing.
Bubble plots show the RRBS sequences aligned to a DMR (chr14:99765624-99765704) (top) and the traditional bisulfite sequencing data generated from the same locus (bottom). Each row shows the methylation status of the 5 CpG sites within this region (black and gray circles stand for methylated and unmethylated cytosines). The average methylation levels are shown in parentheses. The red * symbol denotes a p-value<0.05 for a binomial test of differential methylation for that site between CR and CON placentas.

Figure 4: Screenshots of DNA methylation tracks at **A.** *ptger1*, **B.** *inpp5f*, and **C.** *microRNA 149.* Gene annotation tracks are on the top, followed by 10 tracks of methylation levels from CR and CON samples, and the DMR tracks on the bottom. The methylation levels at each measured CG site are represented as bars whose length represents methylation levels from 0 to 100%.

Figure 5: Expression level of *ptger1* and *miR-149* between CR and CON groups in all, male, and female samples. The size of biological replicates (n) for each comparison is shown in bracket.

Figure 6: Change of methylation versus change of expression.
A. Boxplots of changes of expression levels in differentially methylated genes between CR and CON, and **B.** between female and male; **C.** Changes of methylation levels in promoters and genes ranked by the change in gene expression level between CR and CON, and **D.** between female and male;

Tables

Table 1: Differentially expressed pathways

Pathway	Total genes in the pathway	Up-regulated in CR	Down-regulated in CR	p-value of enrichment test	Note
Pregnancy specific glycoproteins	16		Psg16 Psg17 Psg18 Psg19 Psg20 Psg21 Psg22 Psg23 Psg25 Psg26 Psg27 Psg28 Psg-ps1	5.46E-16	• Elevated expression in males (p = 4.48E-22) • Facilitate maternal immune tolerance of fetus. • Lower levels have been associated with IUGR, fetal hypoxia, and threatened abortion.
Apolipoproteins	21	Apoa2 Apoc1 Apoc2 Apom Apoe Apob Apoa4 Apoa1		1.45E-6	• Mostly upregulated in males versus females. • Have been implicated with cardiovascular and metabolic disease in adults, and elevated fetal blood levels of one, ApoB, have already been associated with IUGR and adult atherosclerosis
Fatty Acid Binding Proteins	7	Fabp4 Fabp5		0.03	• Maternal-fetal lipid exchange • Cardiovascular and metabolic disease
Cathepsins and Granzymes	27	Ctss Ctsh	Cts3 Ctsm Gzmf Gzmd Ctsk Gzmg Gzmc Gzme	1.90E-8	• Granzymes have higher expression in males. (p = 2.82E-8) • Potential role in trophoblast invasion

p-value calculated from the hyergeometric test of enrichment

Table 2: Differentially methylated genes and enriched gene networks

Comparison	DMR	Differentially methylated genes	Top major networks (significance score=-log10 (p-value))
CR vs. CON	477	297	▪ Nervous System Development and Function, Embryonic Development, Organ Development (41) ▪ Cardiovascular System Development and Function, Cellular Movement, Embryonic Development (36) ▪ Cellular Assembly and Organization, Cellular Function and Maintenance, Cellular Movement (32) ▪ Cell-To-Cell Signaling and Interaction, Developmental Disorder, Endocrine System Disorders (31) ▪ Cardiovascular System Development and Function, Tissue Development, Protein Synthesis (27)
CR vs. CON (with sex effect)	1141	667	▪ Cellular Development, Nervous System Development and Function, Visual System Development and Function (49) ▪ Cellular Function and Maintenance, Auditory and Vestibular System Development and Function, Organ Morphology (41) ▪ Cell Signaling, Nucleic Acid Metabolism, Small Molecule Biochemistry (41) ▪ Cancer, Endocrine System Disorders, Gastrointestinal Disease (37) ▪ Tissue Morphology, Connective Tissue Development and Function, Embryonic Development (37)
CR vs. CON (female)	881	459	▪ Connective Tissue Development and Function, Connective Tissue Disorders, Dermatological Diseases and Conditions (43) ▪ Cell Signaling, Molecular Transport, Vitamin and Mineral Metabolism (41) ▪ Cellular Assembly and Organization, Cellular Compromise, Embryonic Development (38) ▪ Cell Signaling, Connective Tissue Disorders, Dental Disease (32) ▪ Cellular Assembly and Organization, Cellular Compromise, Carbohydrate Metabolism (28)
CR vs. CON (male)	892	477	▪ Connective Tissue Development and Function, Embryonic Development, Organ Development (43) ▪ Endocrine System Development and Function, Molecular Transport, Small Molecule Biochemistry (36) ▪ Digestive System Development and Function, Embryonic Development, Endocrine System Development and Function (36) ▪ Cell Morphology, Hematological System Development and Function, Cell-To-Cell Signaling and Interaction (31) ▪ Cellular Function and Maintenance, Molecular Transport, Cell-To-Cell Signaling and Interaction (29)
Female vs. Male	855	572 (413 from autosome, 114 from chrX)	▪ Cellular Assembly and Organization, Cellular Function and Maintenance, Cellular Compromise (45) ▪ Embryonic Development, Organismal Development, Skeletal and Muscular System Development and Function (45) ▪ Developmental Disorder, Skeletal and Muscular Disorders, Hereditary Disorder (42) ▪ Cell Cycle, Organismal Development, Auditory Disease (33) ▪ Cell Death and Survival, Cellular Function and Maintenance, Cell Cycle (31)

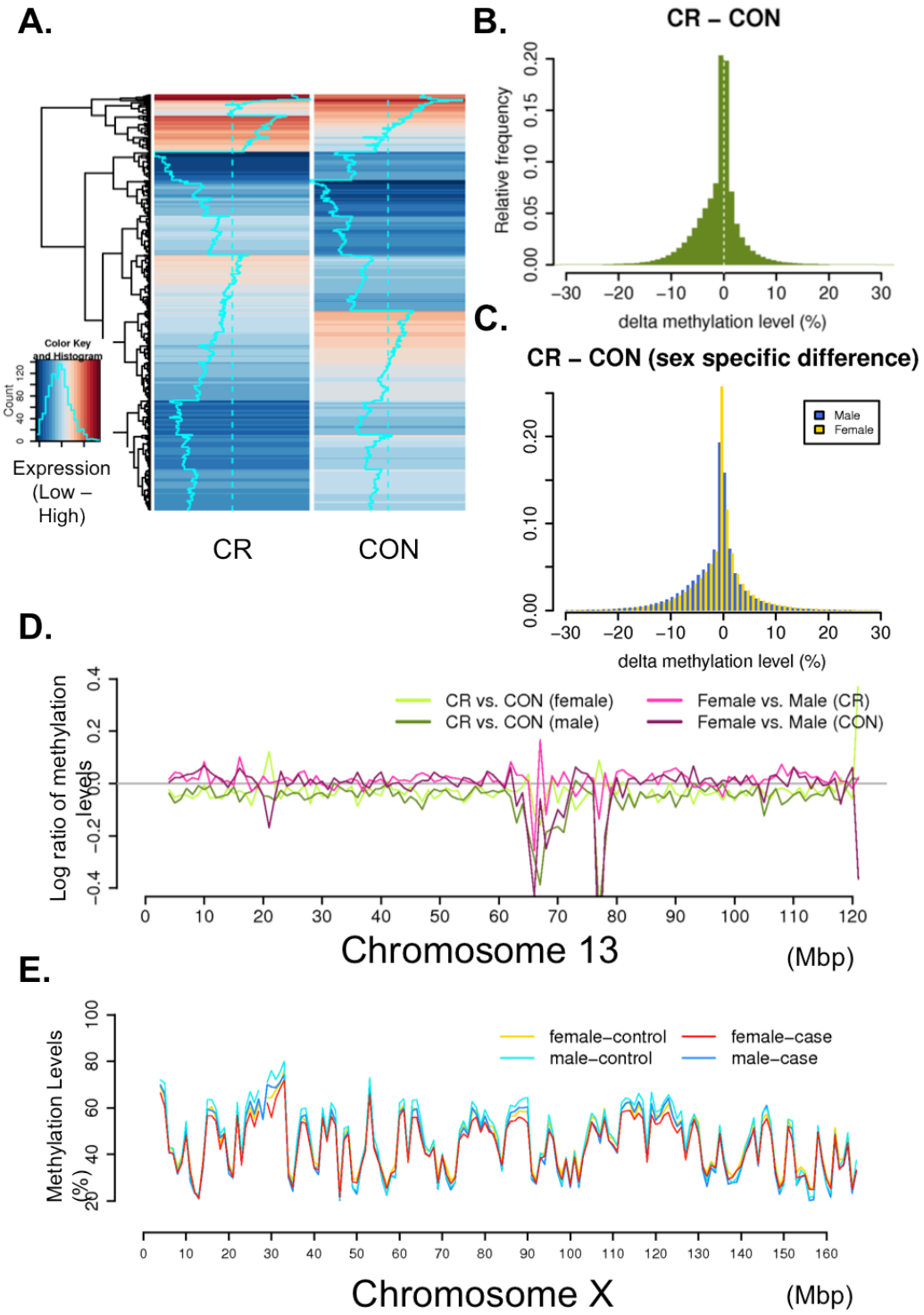

Figure 1 Comparisons of gene expression and DNA methylation levels in mouse placenta samples. **A.** heatmap of gene expression levels in caloric restricted (CR), and wild type (CON) groups (CR); **B.** Average methylation levels in CR vs. CON; **C.** histogram of Δ methylation levels per CG site between CR and CON; **D.** Log2 ratios of methylation levels between sample groups in genome wide view, and **E.** in chromosome 13.

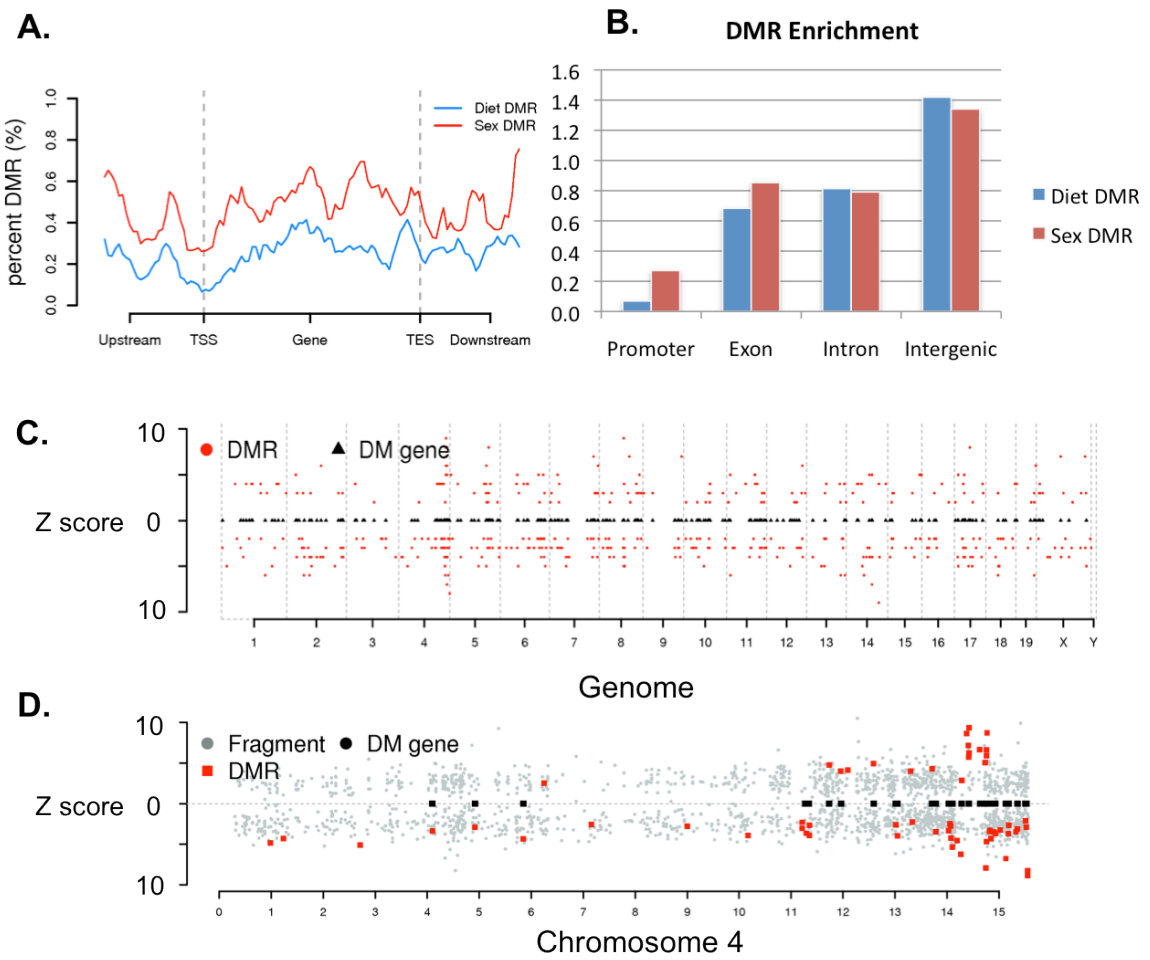

Figure 2 Distribution of differentially methylated regions (DMR), and genes
A. Meta gene plot of percent DMR of RRBS fragments, **B.** Fold enrichment of DMR in promoters, exons, introns, and intergenic regions, **C.** distribution of DMR and the associated genes in genome wide view, and **D.** in chromosome 4; circles are all candidate regions with the z-scores in y axis, squares are the differentially methylated genes associated to DMR (red circles).

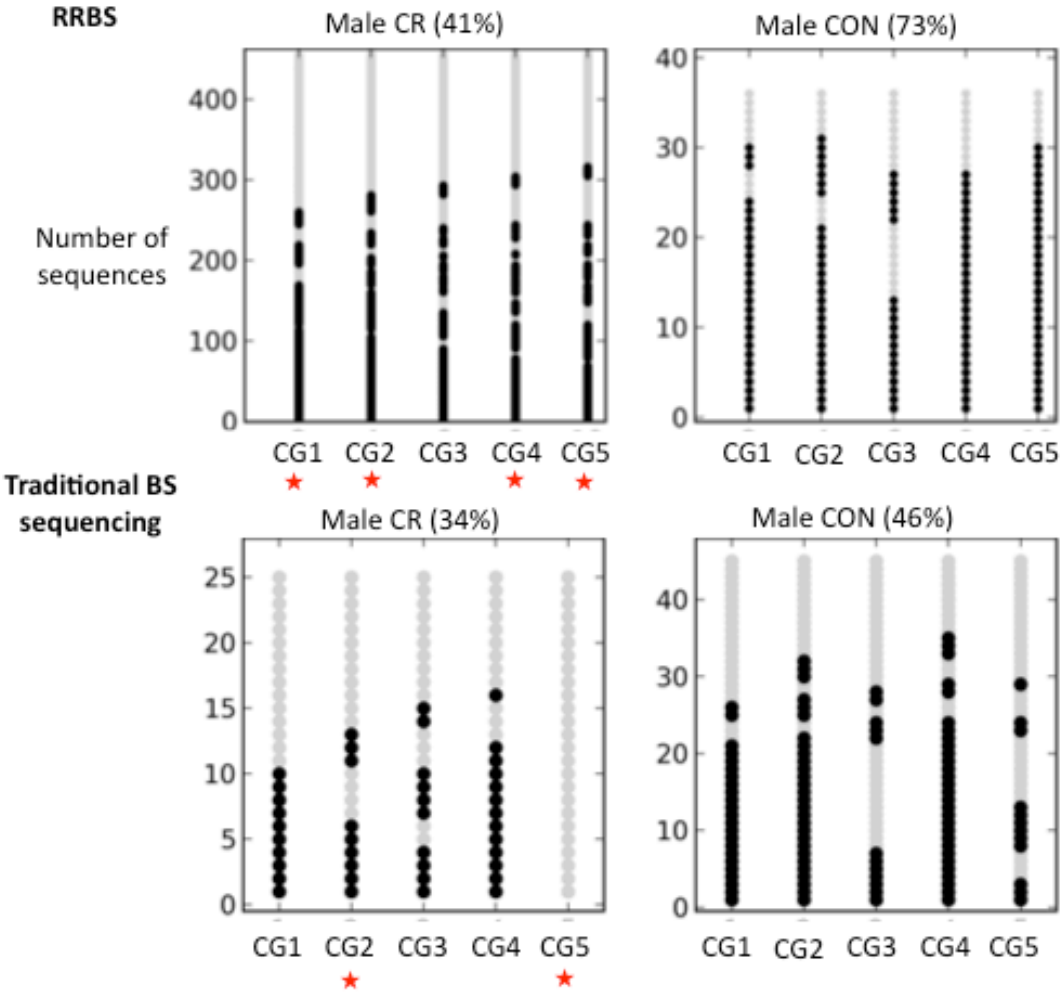

Figure 3: DMR validation using traditional bisulfite sequencing.
Bubble plots show the RRBS sequences aligned to a DMR (chr14:99765624-99765704) (top) and the traditional bisulfite sequencing data generated from the same locus (bottom). Each row shows the methylation status of the 5 CpG sites within this region (black and gray circles stand for methylated and unmethylated cytosines). The average methylation levels are shown in parentheses. The red * symbol denotes a p-value<0.05 for a binomial test of differential methylation for that site between CR and CON placentas.

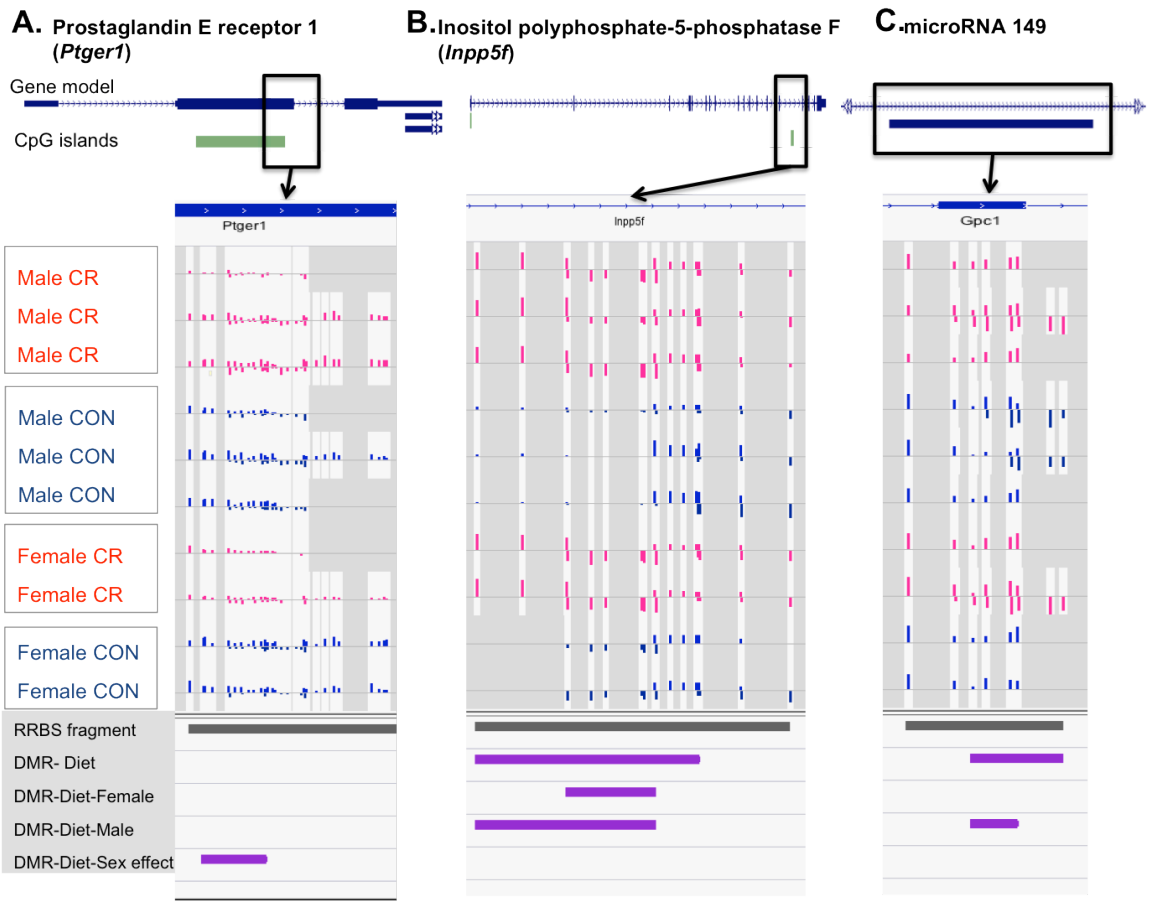

Figure 4: Screenshots of DNA methylation tracks at **A.** *ptger1*, **B.** *inpp5f*, and **C.** *microRNA 149.*

The gene annotation tracks are on the top, followed by 10 tracks of methylation levels from CR and CON, and the DMR track in the bottom. The methylation levels at each measured CG sites are presented as bars with length representing methylation level from 0 to 100%.

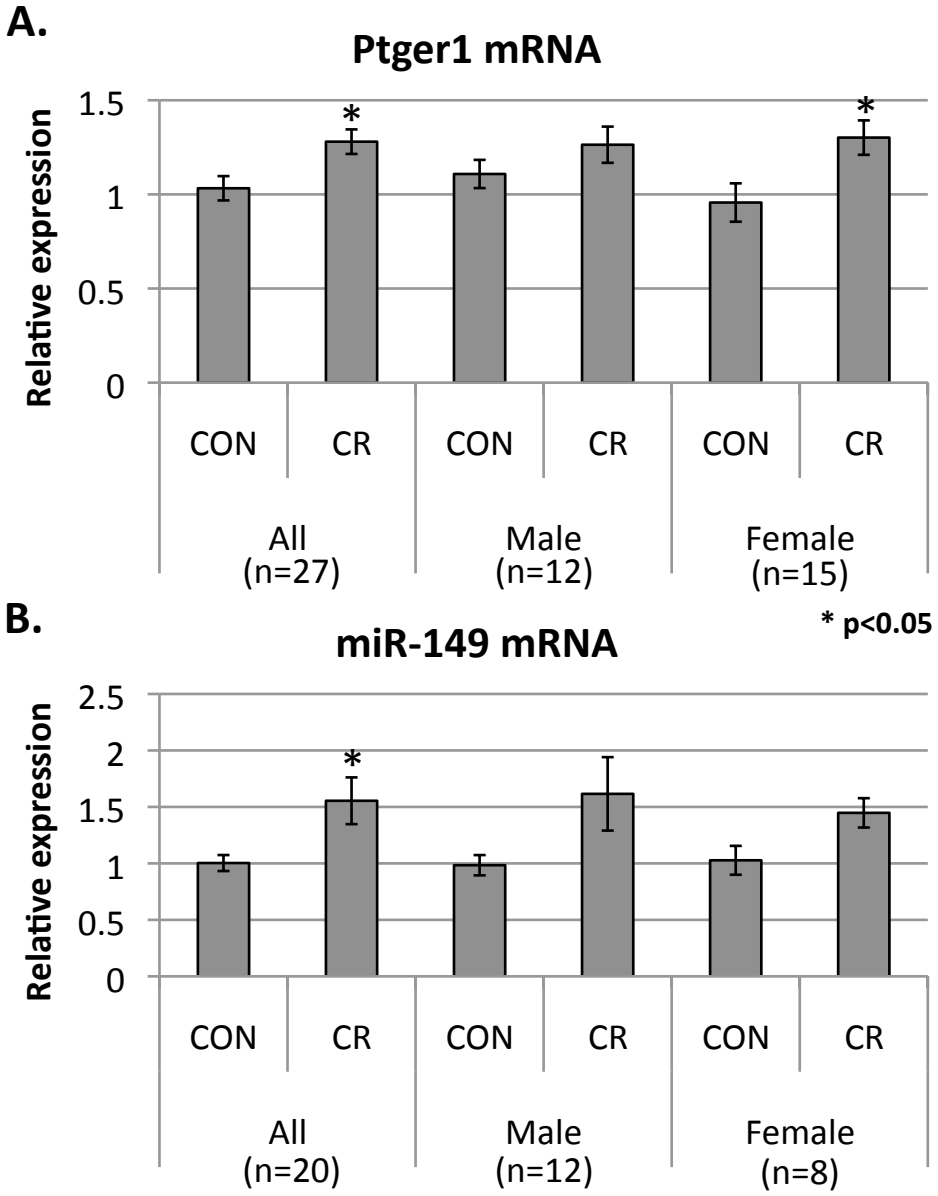

Figure 5: Expression level of *ptger1* and *miR-149* between CR and CON groups in all, male, and female samples. The size of biological replicates (n) for each comparison is shown in bracket.

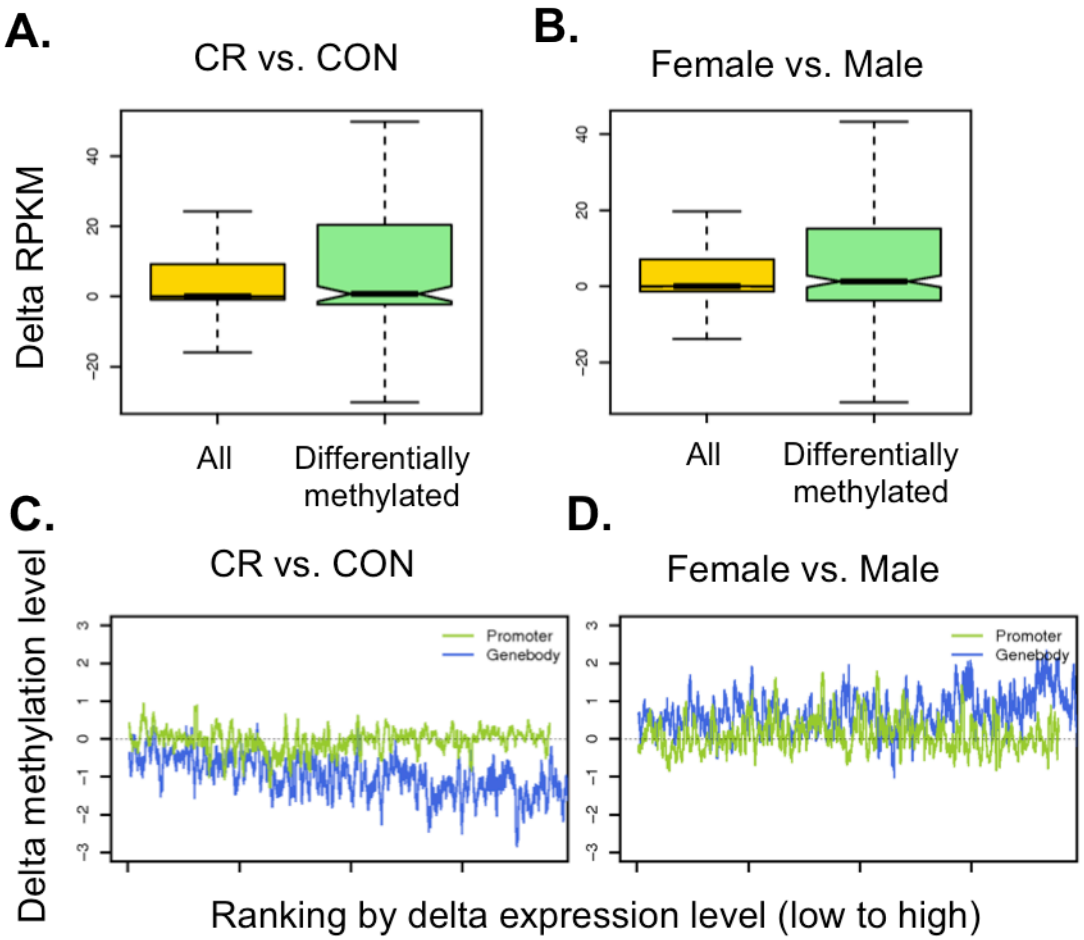

Figure 6: Change of methylation versus change of expression.
A. Boxplots of changes of expression levels in differentially methylated genes between CR and CON, and **B.** between female and male; **C.** Changes of methylation levels in promoters and genes ranked by the change in gene expression level between CR and CON, and **D.** between female and male;